



A Journal of the Gesellschaft Deutscher Chemiker

Angewandte Chemie

GDCh

International Edition

www.angewandte.org

Accepted Article

Title: Host–Guest Chemistry Within Cellulose Nanocrystal Gel Receptors

Authors: Dongjie Zhang, Miguel Soto, Lev Lewis, Wadood Hamad, and Mark MacLachlan

This manuscript has been accepted after peer review and appears as an Accepted Article online prior to editing, proofing, and formal publication of the final Version of Record (VoR). This work is currently citable by using the Digital Object Identifier (DOI) given below. The VoR will be published online in Early View as soon as possible and may be different to this Accepted Article as a result of editing. Readers should obtain the VoR from the journal website shown below when it is published to ensure accuracy of information. The authors are responsible for the content of this Accepted Article.

To be cited as: *Angew. Chem. Int. Ed.* 10.1002/anie.201913030
Angew. Chem. 10.1002/ange.201913030

Link to VoR: <http://dx.doi.org/10.1002/anie.201913030>
<http://dx.doi.org/10.1002/ange.201913030>

Host–Guest Chemistry Within Cellulose Nanocrystal Gel Receptors

Dongjie Zhang,^{†‡±} Miguel A. Soto,^{†±} Lev Lewis,[†] Wadood Y. Hamad,[§] and Mark J. MacLachlan^{*†||±}

[†] Department of Chemistry, University of British Columbia, 2036 Main Mall, Vancouver, British Columbia V6T 1Z1, Canada

[‡] MIT Key Laboratory of Critical Materials Technology for New Energy Conversion and Storage, School of Chemistry and Chemical Engineering, Harbin Institute of Technology, Harbin 150001, P. R. China

[§] Transformation and Interfaces Group, Bioproducts Innovation Centre of Excellence, FPInnovations, 2665 East Mall, Vancouver, British Columbia V6T 1Z4, Canada

^{||} Quantum Matter Institute, University of British Columbia, 2355 East Mall, Vancouver, British Columbia, V6T 1Z4 Canada

[±] WPI Nano Life Science Institute, Kanazawa University, Kanazawa, 920-1192 Japan

[±] These authors contributed equally

Abstract

Cellulose nanocrystals (CNCs) spontaneously assemble into gels when mixed with a polyionic organic or inorganic salt. Here, we have used this ion-induced gelation strategy to create functional CNC gels with a rigid tetracationic macrocycle, cyclobis(paraquat-*p*-phenylene) (**CBPQT**⁴⁺). Addition of [**CBPQT**]Cl₄ to CNCs causes gelation and embeds an active host inside the material. The fabricated CNC gels can reversibly absorb guest molecules from solution then undergo molecular recognition processes that create colorful host–guest complexes. These materials have been implemented in gel chromatography (for guest exchange and separation), and as elements to encode 2- and 3-dimensional patterns. We anticipate that this concept might be extended to design a set of responsive and selective gel-like materials functioning as, for instance, water-pollutant scavengers, substrates for chiral separations, or molecular flasks.

Introduction

Natural and synthetic gels have been known and investigated for centuries. Today, these materials are ubiquitous and are used in diverse applications, spanning from simple food additives^[1] and drug carriers,^[2–4] to intricate smart materials^[5,6] and soft robotics.^[7]

Gels are entangled networks where a fluid is physically confined, yielding a material with a unique soft-solid behavior.^[8] Like other porous materials,^[9–11] gels can

serve as molecular receptors, absorbing chemical species from solution or air.^[12–14] When installing functional units inside a gel structure (*e.g.* a ligand or a molecular host), either chemically or physically, reversible, responsive, and selective absorption processes can occur.^[15–18] Supramolecular approaches to embed functional moieties within gels remain rare.^[19–22]

Cellulose nanocrystals (CNCs) are spindle-shaped particles obtained by the acid (H₂SO₄) hydrolysis of bulk cellulose. This chemical treatment produces nanoparticles that contain sulfate half-ester groups (R–OSO₃[−]) on their surface.^[23] When dispersed in water, CNCs form colloidal suspensions that remain stable because of sulfate–sulfate interparticle repulsions, which are poorly screened by the counterions.^[24,25] These colloids can be disturbed by the addition of inorganic or organic salts, which modifies the ionic strength of the medium and causes gel formation (Figure 1a). This process is spontaneous and entropically-driven,^[26] and has been used by several groups to assemble cellulose-based hydrogels.^[27–31] In fact, there is considerable interest in CNC-based gels as they are attractive materials for separation/purification purposes,^[32] drug-delivery,^[33] sensing,^[34,35] thermal insulation,^[36] tissue engineering,^[37] and 3D printing.^[38]

Here, we present a new methodology to create CNC-based materials that contain functional ions. Specifically, we envisioned ionic macrocycles driving gelation of CNCs to generate materials with embedded host molecules. The gels could function as receptors to absorb guest species from solution to subsequently undergo reversible assembly of host–guest complexes in their interior. A visible macroscale change during the sequential process of guest absorption/self-assembly would also allow for the use of these materials in gel chromatography and guest-conditioned patterning.

Results and Discussion

To pursue this concept, we selected the macrocycle cyclobis(paraquat-*p*-phenylene) (CBPQT⁴⁺) as the functional ion.^[39] This host was chosen based on the following four characteristics: (1) its tetracationic character will facilitate CNC gelation; (2) the salt

solubility can be tuned by appropriate counterion selection; (3) this host has a shape-persistent cavity that will not collapse inside the gels; and (4) **CBPQT**⁴⁺ reversibly binds π -electron-rich guests, such as **G1** and **G2** (Figure 1b), to produce colorful host-guest complexes.^[40–42]

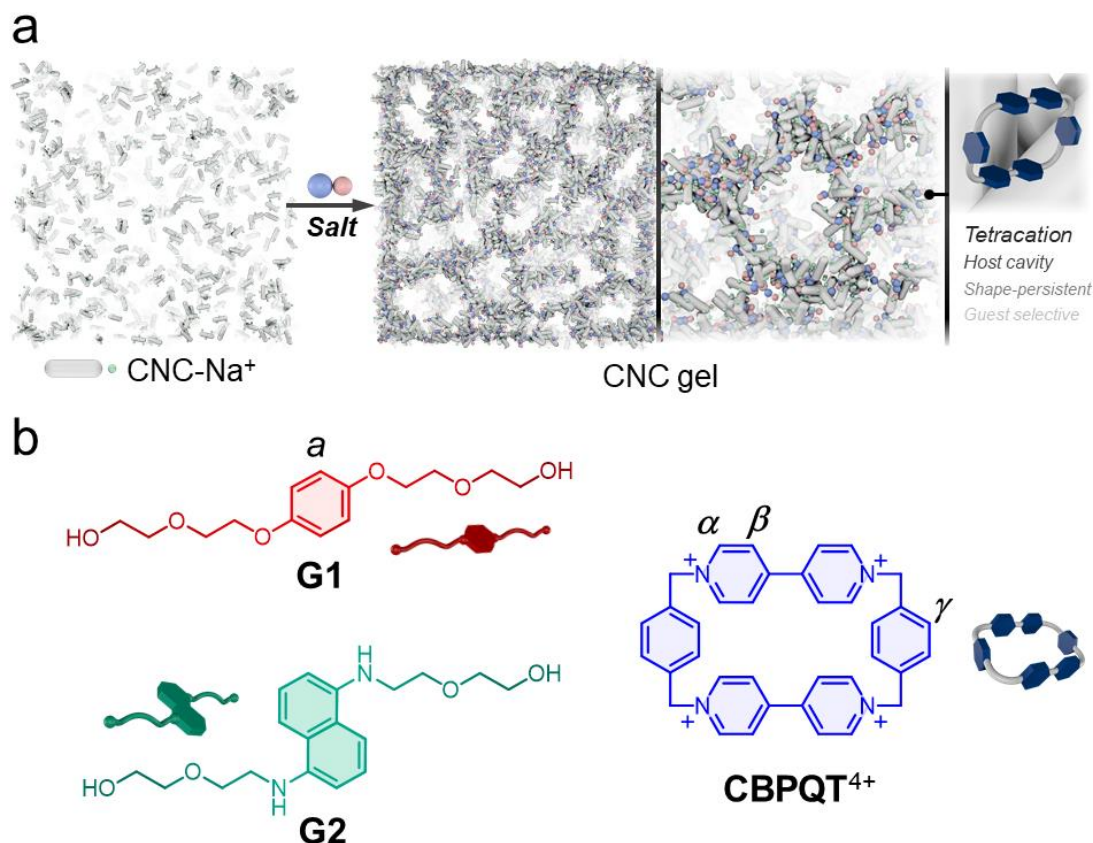


Figure 1. (a) Schematic representation of the ion-induced gelation of CNCs. (b) Chemical structures of the selected host, **CBPQT**⁴⁺, and guest molecules, **G1** and **G2**. Protons assigned in the NMR discussion are labeled in this figure.

We started by mixing an aqueous suspension of sodium-neutralized cellulose nanocrystals (CNC-Na⁺, 6 wt%) with [**CBPQT**]**Cl**₄ in solution. The host concentration was varied from 0.4 to 3.8 mM to generate five independent systems. At a low salt concentration (0.4 and 0.8 mM), the combination of both components, CNC-Na⁺ and **CBPQT**⁴⁺, did not produce a visible change; the samples remained semitransparent and liquid. At higher concentrations (**CBPQT**⁴⁺ at 1.3, 2.5, and 3.8 mM), however, we obtained colorless hydrogels (CNC-**CBPQT**⁴⁺) that were either semitransparent or

opaque (Fig. S1).

From the prepared series of hydrogels, we noticed that low amounts of host (1.3 mM) produced materials with liquid-like behavior, displaying an injectable consistency. Higher concentrations of **CBPQT**⁴⁺ (2.5 and 3.8 mM) generated more robust hydrogels that could be molded and physically manipulated while preserving their shape (Fig. 2a). These observations qualitatively suggest that more robust hydrogels can be produced with increasing the proportion of **CBPQT**⁴⁺.

The enhancement of the gel stiffness with increasing host concentration was confirmed through rheological studies of the CNC-**CBPQT**⁴⁺ systems (see ESI for details). The complex modulus (G^*) of an aqueous suspension of CNCs was 5.1 Pa at an oscillatory frequency of 8.9 rad s⁻¹; addition of a small quantity of [**CBPQT**]_{Cl₄} (0.4 mM) caused a *ca.* 70% increase of G^* , reaching 8.6 Pa. Continuous addition of host led to a concomitant increase of G^* , attaining 17.4 kPa at 3.8 mM of **CBPQT**⁴⁺. This represents a 200-fold increase with respect to our weakest hydrogel, prepared at 1.3 mM of **CBPQT**⁴⁺ ($G^* = 63.2$ Pa, see Fig. S2 and Table S1).

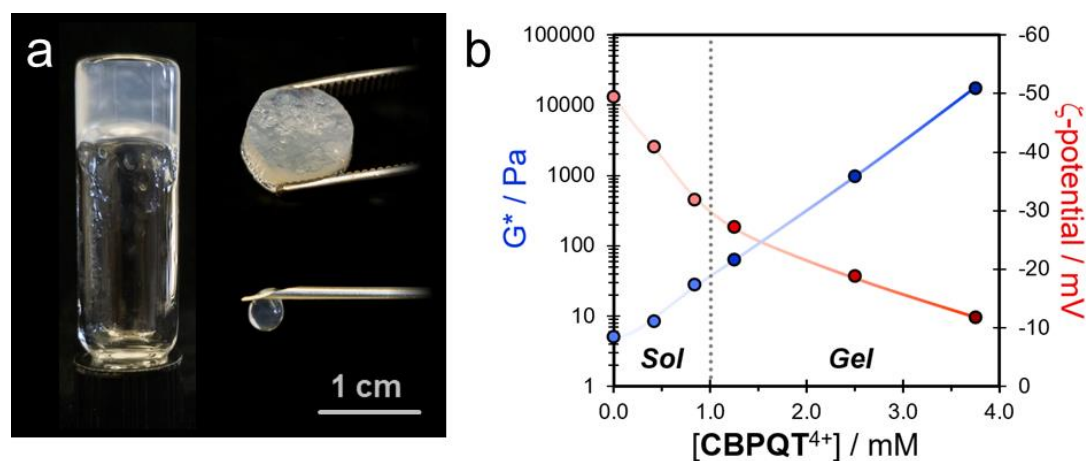


Figure 2. (a) Photographs of CNC-**CBPQT**⁴⁺ hydrogels at varied concentrations of [**CBPQT**]_{Cl₄}: 1.3 mM (injectable viscous liquid), 2.5 mM (inverted vial), and 3.8 mM (disc-shaped gel). (b) Changes of the complex viscoelastic modulus (G^*) and ζ -potential plotted as functions of [**CBPQT**]_{Cl₄} concentration. Solid curves depict the observed trends. The discontinuous line at 1.0 mM differentiates between the liquid and gel states of the CNC-**CBPQT**⁴⁺ system.

Similarly, we assessed the change in surface potential of dispersed CNCs when combined with the tetracationic host. By ζ -potential analyses, we found a value of -49.4

mV for a pristine CNC-Na⁺ dispersion, indicating that sodium ions poorly screen the negative surface charge of the nanocrystals, yielding a stable aqueous suspension. The addition of **CBPQT**⁴⁺ (1.25 mM) to generate CNC-**CBPQT**⁴⁺ increased the ζ -potential, reaching a value of -27.2 mV (Fig. 2b). With an increase of **CBPQT**⁴⁺ (3.8 mM) the potential further increased to -11.8 mV (Table S2). These results show that the tetracation effectively shields the CNCs surface charge, even under dilute conditions (0.4 mM, ζ -potential = -41.0 mV), driving the aggregation of nanocrystals and the subsequent formation of hydrogels with different mechanical strengths.

We anticipated that the prepared hydrogels could function as guest receptors in aqueous media. Despite their apparent sturdiness, however, we observed that all gels lost cohesion when immersed in water, and eventually collapsed (see Fig. S3). This could be ascribed to the leaching of [**CBPQT**]Cl₄ that leads to the redispersion of CNCs. To address this, we employed a less polar medium composed of ethanol:water (3:1), in which [**CBPQT**]Cl₄ is poorly soluble. In this medium, our materials did not collapse even after one week of storage. The ability of the CNC-**CBPQT**⁴⁺ gels (**CBPQT**⁴⁺ at 3.8 mM) to act as guest receptors was thus evaluated in an ethanol/water solvent system.

Host **CBPQT**⁴⁺ can accommodate guests **G1** or **G2** in its cavity, as thoroughly documented by Stoddart's group.^[43,44] The assembly process has been reported in non-competitive organic media, such as acetonitrile or acetone, but rarely explored in water.^[45] We found that host **CBPQT**⁴⁺ rapidly self-assembles with **G1** and **G2** in ethanol/water solution to generate pseudorotaxane complexes with a 1:1 stoichiometry (see Fig. S4–S7). Both complexes, named hereafter as **G1**⊂**CBPQT**⁴⁺ and **G2**⊂**CBPQT**⁴⁺, differ in two aspects. First, they have different colors: **G1**⊂**CBPQT**⁴⁺ is orange (λ_{\max} = 460 nm) while **G2**⊂**CBPQT**⁴⁺ is green in solution (λ_{\max} = 706 nm). Second, they have different stability (Fig. S8), as measured by the equilibrium constant (K_a) and estimated as $(1.3 \pm 0.1) \times 10^3 \text{ M}^{-1}$ and $(4.3 \pm 0.2) \times 10^4 \text{ M}^{-1}$ for **G1**⊂**CBPQT**⁴⁺ and **G2**⊂**CBPQT**⁴⁺, respectively.

We rationalized that both factors, color and affinity, would prevail when employing the CNC-**CBPQT**⁴⁺ gels as receptors in a dual-phase (gel/solution) system. To prove this, we fabricated a ~500 μL disc-shaped gel (**CBPQT**⁴⁺ at 3.8 mM), followed by its

solvent exchange from water to ethanol/water (see ESI). The obtained CNC-CBPQT^{4+} gel was immersed in a colorless solution of **G1** (25 mM, 5 mL) and kept at 25 °C. After a few minutes, the surface of the material turned into orange while the interior remained white; the colored portion gradually extended along the disc until, after *ca.* one hour, the whole gel was uniformly orange (Fig. 3a). This macroscopic observation suggests that as the diffusion process occurs, **G1** permeates into the gel structure where it encounters the embedded CBPQT^{4+} units. Then both species, being close in proximity, undergo molecular recognition to yield pseudorotaxane $\text{G1} \subset \text{CBPQT}^{4+}$ inside the gel, which is unveiled by its intense orange color.

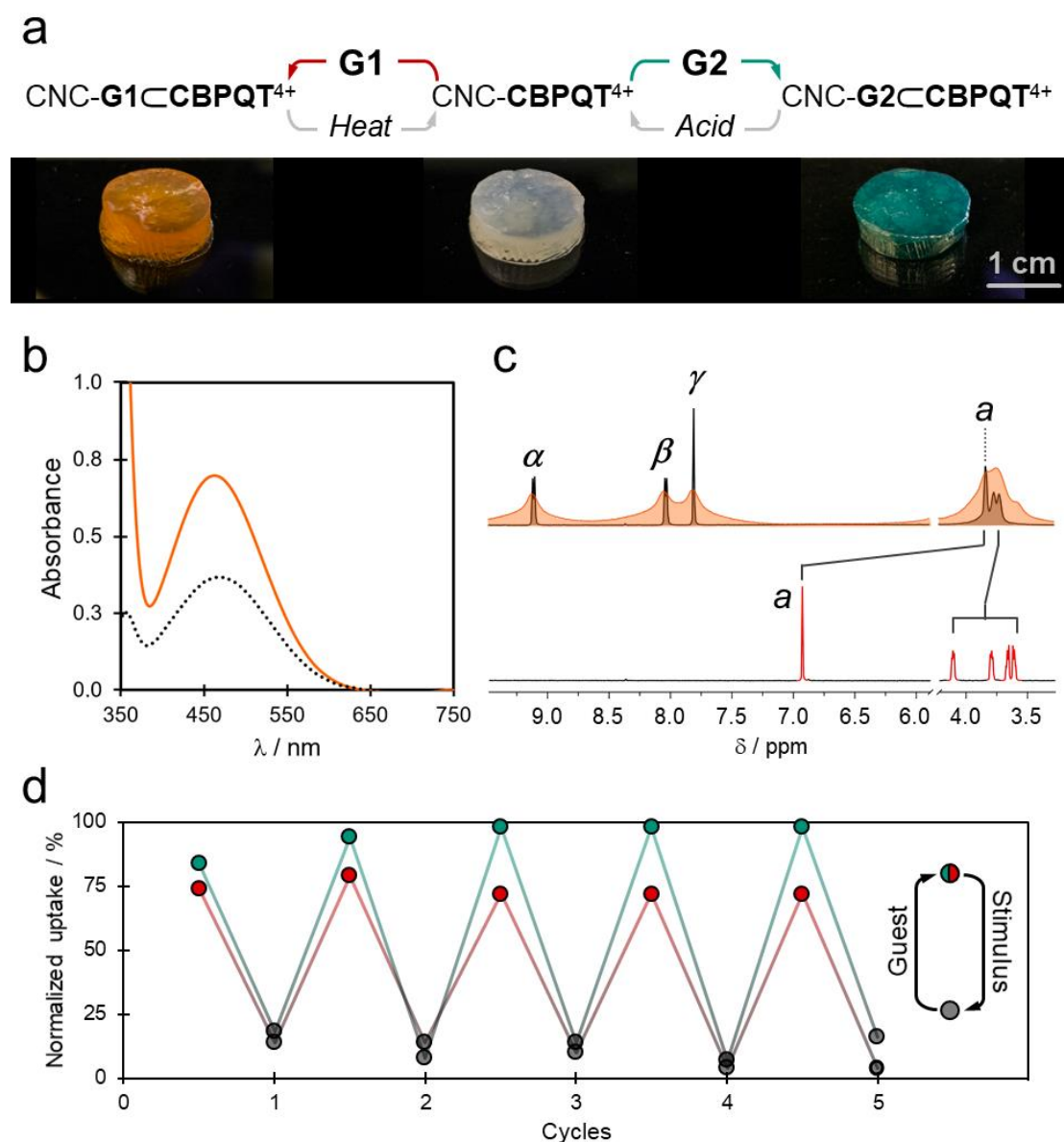


Figure 3. (a) Assembly of in-gel pseudorotaxanes. From left to right, photographs of $\text{CNC-G1} \subset \text{CBPQT}^{4+}$,

CNC-**CBPQT**⁴⁺, and CNC-**G2**⊂**CBPQT**⁴⁺ gels. (b) UV-vis spectra (3:1 ethanol/water) of **G1**⊂**CBPQT**⁴⁺ complex within gel (dashed line) and in solution (bold line).^[46] (c) ¹H NMR spectra (400 MHz, D₂O) of pseudorotaxane **G1**⊂**CBPQT**⁴⁺ (top) gel (orange) and solution (black). **G1** guest (bottom). (d) Absorption/desorption cycles, using heat (red) and acid (green) stimuli, measured by ¹H NMR spectroscopy. Guest concentration was determined from solution before and after immersing a gel receptor. Uptake is normalized by the concentration of embedded host (3.8 mM = 100%). **G1** and **G2** shown in red and green, respectively.

A UV-vis spectrum of the gel CNC-**G1**⊂**CBPQT**⁴⁺ resembles the spectrum of **G1**⊂**CBPQT**⁴⁺ in solution, with an absorption band at 460 nm (Fig. 3b). This result is in good agreement with the formation of a charge-transfer complex between the electron-poor paraquat moieties of the host and the electron-rich phenylene core of **G1**.

We also confirmed the self-assembly of the in-gel **G1**⊂**CBPQT**⁴⁺ complex by ¹H NMR spectroscopy. Figure 3c shows the ¹H NMR spectrum of the resulting CNC-**G1**⊂**CBPQT**⁴⁺ gel (see ESI for sample preparation). Interestingly, all resonances compare well with the signals assigned to **G1**⊂**CBPQT**⁴⁺ in solution, although with significant broadening. All the aromatic host resonances (α , β , and γ) show a slight shift with respect to CNC-**CBPQT**⁴⁺ (Fig. S11); for instance, β exhibits a $\Delta\delta_{\beta} = -0.2$ ppm. More noticeably, the phenylene protons (a) of **G1** present an upfield shift of 3.2 ppm compared to a pure solution of the guest. This dramatic shift can be explained by the shielding of the **G1** core while it is inside the host cavity, as in a pseudorotaxane complex. Together, the UV-vis and NMR data verify formation of a pseudorotaxane host-guest complex inside the gel CNC-**CBPQT**⁴⁺ upon introducing guest **G1**.

The second guest selected, **G2**, yielded analogous results with only one difference: the apparent color. Following the diffusion-driven self-assembly of CNC-**G2**⊂**CBPQT**⁴⁺, the disc-shaped gels became green (Fig. 3a), showing an absorbance band at 706 nm in the UV-vis spectrum (Fig. S10). ¹H NMR spectroscopy confirmed the formation of pseudorotaxane within the gel by comparison with the self-assembly of **G2**⊂**CBPQT**⁴⁺ in solution (Fig. S11). Of note, other properties of the gels, *e.g.* stiffness and ζ -potential, were unresponsive to the presence of **G1** or **G2** (Fig. S12 and Tables S3/S4). For instance, the difference in ζ -potential between CNC-**CBPQT**⁴⁺ and CNC-**G1**⊂**CBPQT**⁴⁺ is only 0.6 mV (Table S4). We rationalize that the neutral

charge of **G1** and **G2**, and their relatively small sizes, do not generate a significant effect on the ion–ion interactions that hold the CNC–CBPQT⁴⁺ gel components together.

In principle, the formation of both in-gel pseudorotaxanes could be reversed by disrupting the noncovalent interactions that hold host and guest together. We therefore explored their controlled dissociation by employing physical and chemical stimuli.

A CNC-**G1**–CBPQT⁴⁺ gel was immersed in an ethanol/water mixture and maintained at room temperature for one hour. Within this period, no visible changes were observed. Heating the system at 60 °C caused the orange color to fade and, after *ca.* one hour, the disc-shaped material turned homogeneously white. This color change indicates that the thermal stimulus promotes the dissociation of **G1** from the host cavity. At this point, the exclusion of **G1** from the gel was not ensured, so heating was continued for four hours in fresh ethanol/water. Both phases, gel and solution, were separated. Noteworthy, the isolated gel did not recuperate its original orange color, whereas the recovered solution, analyzed by ¹H NMR spectroscopy (Fig. S13), contained only compound **G1**.

Disassembly of CNC-**G2**–CBPQT⁴⁺ was also accomplished. By immersing the CNC-**G2**–CBPQT⁴⁺ gel in an acidic solution (3 M HCl, 2 mL), the gel visibly changed color from green to white in *ca.* one hour. After keeping the gels submerged in the acidic solution for about four hours, we recovered [**G2**·H₂]²⁺ in solution (Fig. S14 for ¹H NMR data), and CNC-CBPQT⁴⁺ as a white gel. We ascribe this dissociation to the protonation of **G2** within the material, which yields [**G2**·H₂]²⁺. This species formed inside the gel is expected to repel the tetracationic host and escape from its cavity.

Furthermore, we demonstrated that using the appropriate stimulus (heat for **G1** or acid for **G2**), CNC-CBPQT⁴⁺ gels can reversibly uptake **G1** and **G2** up to five times without significant decay, as shown in Figure 3d. Interestingly, the ratio of absorbed guest varies between **G1** and **G2** by *ca.* 25%. This might be explained by the difference in affinity between the host and both guests; in solution, CBPQT⁴⁺ binds stronger to **G2** than to **G1**. We also proved that a CNC-CBPQT⁴⁺ gel absorbs non-active guests, such as tetraethylene glycol monotosylate (**M1**) (Fig. S19). However, the amount of **M1** absorbed was just 45% with respect to the **G2** uptake. (All experiments were

performed at same concentrations of **G1**, **G2** and **M1**.)

These observations confirm that the amount of absorbed (and complexed) guests depends on the intercomponent affinity. Nevertheless, and if needed, the absorption capacity of the receptors can be tuned by modifying the ratio of embedded host. For example, a material prepared with **CBPQT**⁴⁺ at 7.5 mM can uptake about twice the amount of **G1** absorbed by a gel assembled with 3.8 mM of host (Fig. S15).

Following the analysis of the in-gel host–guest complexes, we sought to take advantage of the contrasting affinity and apparent color of the pseudorotaxanes by implementing the **CNC-CBPQT**⁴⁺ materials in gel chromatography for exchange and separation purposes. To investigate this, a solvent-exchanged **CNC-CBPQT**⁴⁺ gel was transferred into a glass pipette, then a solution of **G1** (25 mM) was passed through the packed column, which gradually turned orange accordingly with the diffusion of **G1**. Although the stationary phase appeared intensely orange (Fig 4a), the collected solution remained colorless, indicating that **CBPQT**⁴⁺ did not leach out along with the guest. A ¹H NMR spectrum of the collected solution showed exclusively the expected resonances for **G1** (Fig 4b).

Eluting a solution of **G2** (10 mM) through the same column produced guest-exchange, so that the stationary phase slowly changed color, from orange to green, as **G2** displaced **G1** from the host cavity. During the exchange process, **G1** was identified by ¹H NMR spectroscopy of the collected eluent and, when completed, **G2** was solely observed (Fig. 4b). To regenerate the stationary phase, we treated the column with an acidic solution (50 mM HCl). This caused protonation of **G2** and its exclusion from the host (and from the stationary phase), accompanied by a color change (Fig 4a). The generated cation [**G2**·H₂]²⁺ was recovered from the column and unequivocally identified by ¹H NMR spectroscopy (Fig. 4b). Further treatment of the stationary phase with ethanol/water allowed for its pH neutralization. No other components were noticed in the collected solvent.

Analogously, we attempted the purification of a **G1/G2** mixture through gel column chromatography. For this, a stationary phase was made with silica gel (SiO₂) and **CNC-CBPQT**⁴⁺ in a 1:1 volume ratio. SiO₂ provided structural support to the

CNC-CBPQT⁴⁺ gels so that a packed column could operate under pressurized conditions. The recurrent ethanol/water solvent system was employed as eluent. After loading the **G1/G2** mixture (1:2 molar ratio),^[47] a light-green color quickly developed at the column baseline (Fig. 4c). As elution progressed, the colored baseline slowly separated into two components that appeared orange and green in color. The orange component, assigned to the in-gel pseudorotaxane **G1**⊂CBPQT⁴⁺, moved faster within the stationary phase, while the green component (in-gel **G2**⊂CBPQT⁴⁺) was left behind (Fig. 4c). This difference relies, like in regular chromatographic separations, on analyte-stationary phase affinity; for our system $K_a(\text{G2} \subset \text{CBPQT}^{4+}) > K_a(\text{G1} \subset \text{CBPQT}^{4+})$. Once the stationary phase became colorless, we assumed that separation was completed (Fig. S20). All collected fractions, recovered as colorless solutions, were evaporated and analyzed by ¹H NMR spectroscopy. In the resulting spectra (Fig. 4d), resonances for **G1** and **G2** were identified in separate fractions, whereas CBPQT⁴⁺ was not detected.

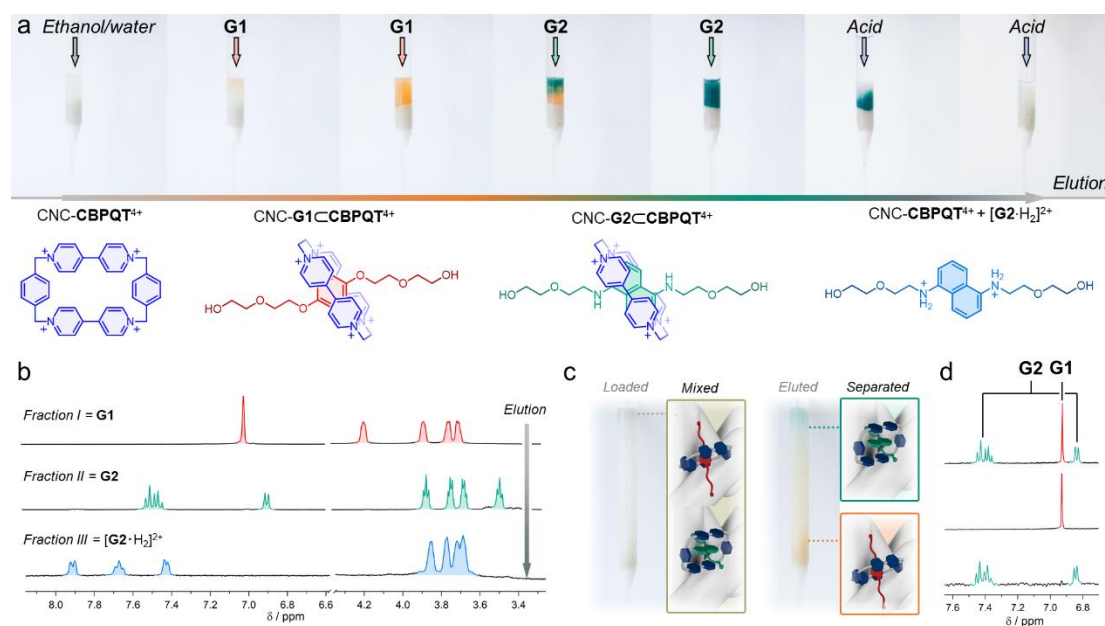


Figure 4. (a) Exchange chromatography. Photographs showing the observed changes as elution progresses (top). Structures of the expected species and complexes present at each stage (bottom). (b) ¹H NMR spectra (400 MHz, D₂O) of selected fractions collected throughout the exchange process. (c) Chromatographic separation of a **G1/G2** mixture. Images showing loaded (left) and partially eluted (right) stages; schematic representations of the complexes are included. (d) ¹H NMR spectra (400 MHz, D₂O) of the **G1/G2** mixture (top) and the components **G1** (middle) and **G2** (bottom) separated by column chromatography.

Furthermore, we envisaged that color changes yielded by in-gel pseudorotaxanes

could be used to encode patterns into 2D and 3D structures (Fig. S22). For this, we used a CNC-CBPQT⁴⁺ gel as the active patterning component while an analogous CNC-PQT²⁺ gel was used as background (PQT²⁺ = methylviologen cation). Beforehand, we confirmed that PQT²⁺ does not self-assemble with G1 or G2 (Fig. S16), and therefore when CNC-PQT²⁺ absorbs G1 or G2 from solution, it does not form a colorful complex.

To encode a pattern, CNC-CBPQT⁴⁺ was cast onto a glass substrate and shaped into a design; this was coated with the background gel to produce a homogeneous surface (Fig. 5a). The generated material was then immersed in a solution of G2. As the guest permeated into the material, a green color gradually appeared in localized regions, until the pattern was fully intelligible. After submerging the material into an acidic solution (3M HCl), the pattern was completely erased, recovering the unreadable 2D surface. This demonstrates the opportunity to use the molecular recognition capability of CNC-CBPQT⁴⁺ for covert encryption.

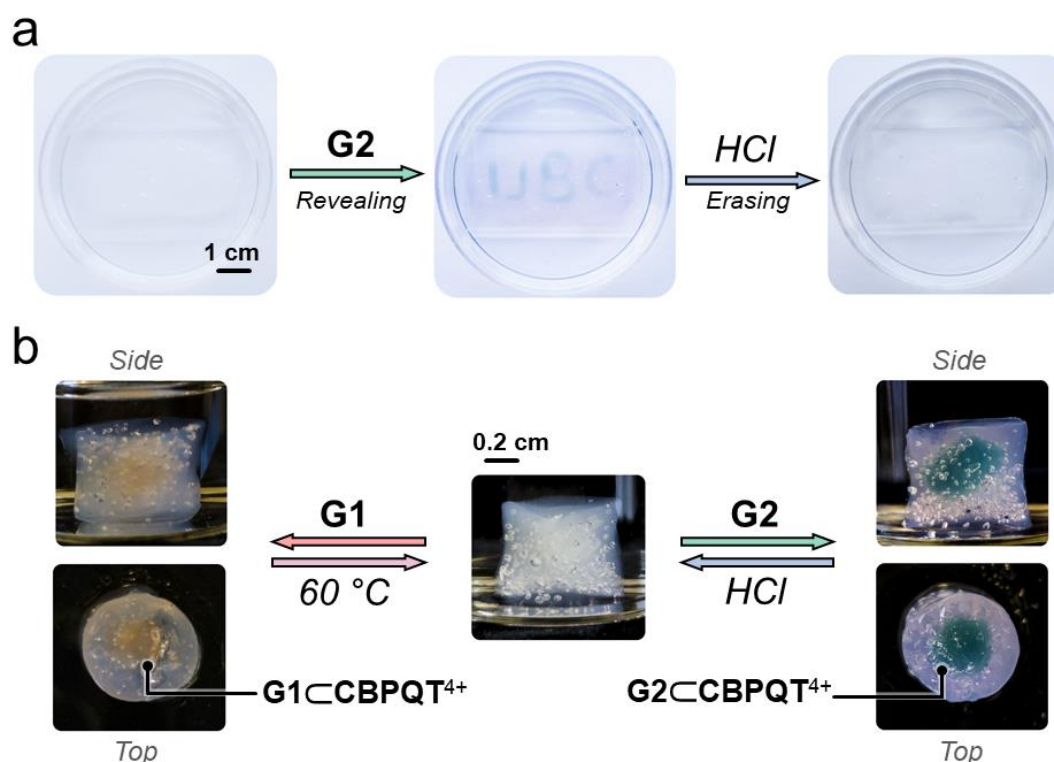


Figure 5. (a) 2D patterning exposure (by G2) and erasing (through G2 protonation). (b) 3D-patterned objects revealed by exposure to G1 (left) and G2 (right). The observed air bubbles were unintentionally trapped within the materials during gelation.

Similarly, we fabricated a 3D-patterned object. For this, a cube-shaped CNC-CBPQT⁴⁺ gel was located within a cylindrical CNC-PQT²⁺ gel. After exposing the system to solutions of **G1** or **G2**, only the embedded cube component became colored (Fig. 5b). This implies that the guests travel through the CNC-PQT²⁺ gel without undergoing any molecular recognition, but as they encounter CNC-CBPQT⁴⁺ the in-gel pseudorotaxanes are formed, turning on a color and revealing the patterned shape. We also proved that the 3D patterns can be successfully erased by applying the appropriate stimulus: heat for **G1** and acid for **G2**.

Conclusions

In summary, we have employed a supramolecular ion-induced strategy to produce CNC-CBPQT⁴⁺ gels with a cationic host embedded in a cellulose nanocrystal matrix. These materials can absorb species from solution, especially electron-rich guests such as **G1** and **G2**, to produce color changes. Interestingly, the guest molecules could be expelled from the host cavity (and from the gel) by applying stimuli, heat for **G1** and acid for **G2**, allowing for the recovery of vacant CNC-CBPQT⁴⁺ receptors. The reversible assembly of in-gel host–guest complexes allowed us to utilize CNC-CBPQT⁴⁺ in gel chromatography for the exchange and separation of **G1** and **G2**. Additionally, the controlled emergence/fading of color was employed to encode 2D and 3D patterns, which are conditioned to the presence of a guest molecule.

We believe that this simple, but robust, gel fabrication strategy might be useful in the future to create new functional materials. The use of polyionic species that trigger gelation and perform a secondary function might be relevant for water remediation, chiral separations, drug-transport/delivery, and chemical reactivity.

Acknowledgments

DZ thanks the Chinese Science Council (CSC) for a scholarship and Professors Yuyan

Liu and Zhongjun Cheng for their support. MAS thanks CONACYT for a postdoctoral fellowship. MJM thanks NSERC for funding (Discovery and CREATE NanoMat grants). The authors acknowledge Prof. Savvas Hatzikiriakos for access to his rheometer.

References

- [1] A. Nazir, A. Asghar, A. Aslam Maan, *Adv. Food Rheol. Its Appl.* **2016**, 8398, 335–353.
- [2] S. W. Kim, B. Jeong, Y. H. Bae, D. S. Lee, *Nature* **1997**, 388, 860–862.
- [3] Y. Qiu, K. Park, *Adv. Drug Deliv. Rev.* **2001**, 53, 321–339.
- [4] C. Karavasili, D. G. Fatouros, *Drug Discov. Today* **2016**, 21, 157–166.
- [5] Z. Wei, J. H. Yang, J. Zhou, F. Xu, M. Zrínyi, P. H. Dussault, Y. Osada, Y. M. Chen, *Chem. Soc. Rev.* **2014**, 43, 8114–8131.
- [6] Z. Qi, C. A. Schalley, *Acc. Chem. Res.* **2014**, 47, 2222–2233.
- [7] L. Hines, K. Petersen, G. Z. Lum, M. Sitti, *Adv. Mater.* **2017**, 29, 1603483.
- [8] J. Zhang, Y. Hu, Y. Li, *Gel Chemistry: Interactions, Structures and Properties*, Springer Singapore, **2018**.
- [9] J.-R. Li, R. J. Kuppler, H.-C. Zhou, *Chem. Soc. Rev.* **2009**, 38, 1477–1504.
- [10] N. Giri, M. G. Del Pópolo, G. Melaugh, R. L. Greenaway, K. Rätzke, T. Koschine, L. Pison, M. F. C. Gomes, A. I. Cooper, S. L. James, *Nature* **2015**, 527, 216.
- [11] K. Jie, Y. Zhou, E. Li, Z. Li, R. Zhao, F. Huang, *J. Am. Chem. Soc.* **2017**, 139, 15320–15323.
- [12] T. Wu, M. Chen, L. Zhang, X. Xu, Y. Liu, J. Yan, W. Wang, J. Gao, *J. Mater. Chem. A* **2013**, 1, 7612–7621.
- [13] F. Jiang, Y. Lo Hsieh, *J. Mater. Chem. A* **2014**, 2, 6337–6342.
- [14] D. M. Alzate-Sánchez, B. J. Smith, A. Alsbaiee, J. P. Hinstroza, W. R. Dichtel, *Chem. Mater.* **2016**, 28, 8340–8346.
- [15] D. Li, Q. Li, N. Bai, H. Dong, D. Mao, *ACS Sustain. Chem. Eng.* **2017**, 5, 5598–5607.
- [16] J. Wang, X. Wang, X. Zhang, *J. Mater. Chem. A* **2017**, 5, 4308–4313.
- [17] S. Zhao, W. J. Malfait, N. Guerrero-Alburquerque, M. M. Koebel, G. Nyström, *Angew. Chem. Int. Ed.* **2018**, 57, 7580–7608.
- [18] D. Zhao, Y. Tian, X. Jing, Y. Lu, G. Zhu, *J. Mater. Chem. A* **2019**, 7, 157–164.
- [19] T. N. Plank, L. P. Skala, J. T. Davis, *Chem. Commun.* **2017**, 53, 6235–6238.
- [20] G.-F. Gong, Y.-Y. Chen, Y.-M. Zhang, Y.-Q. Fan, Q. Zhou, H.-L. Yang, Q.-P. Zhang, H. Yao, T.-B. Wei, Q. Lin, *Soft Matter* **2019**, DOI 10.1039/C9SM01035A.
- [21] B. Li, B. Wang, X. Huang, L. Dai, L. Cui, J. Li, X. Jia, C. Li, *Angew. Chem. Int. Ed.* **2019**, 58, 3885–3889.
- [22] M. Kieffer, A. M. Garcia, C. J. E. Haynes, S. Kralj, D. Iglesias, J. R. Nitschke, S. Marchesan, *Angew. Chem. Int. Ed.* **2019**, 58, 7982–7986.

- [23] Y. Habibi, *Chem. Soc. Rev.* **2014**, *43*, 1519–1542.
- [24] S. Shafeiei-Sabet, W. Y. Hamad, S. G. Hatzikiriakos, *Rheol. Acta* **2013**, *52*, 741–751.
- [25] X. M. Dong, J. F. Revol, D. G. Gray, *Cellulose* **1998**, *5*, 19–32.
- [26] S. Lombardo, A. Gençer, C. Schütz, J. Van Rie, S. Eyley, W. Thielemans, *Biomacromolecules* **2019**, DOI 10.1021/acs.biomac.9b00755.
- [27] H. Dong, J. F. Snyder, K. S. Williams, J. W. Andzelm, *Biomacromolecules* **2013**, *14*, 3338–3345.
- [28] S. Shafeiei-Sabet, W. Y. Hamad, S. G. Hatzikiriakos, *Cellulose* **2014**, *21*, 3347–3359.
- [29] M. Chau, S. E. Sriskandha, D. Pichugin, H. Thérien-Aubin, D. Nykypanchuk, G. Chauve, M. Méthot, J. Bouchard, O. Gang, E. Kumacheva, *Biomacromolecules* **2015**, *16*, 2455–2462.
- [30] P. Bertsch, S. Isabettoni, P. Fischer, *Biomacromolecules* **2017**, *18*, 4060–4066.
- [31] A. L. Oechsle, L. Lewis, W. Y. Hamad, S. G. Hatzikiriakos, M. J. MacLachlan, *Chem. Mater.* **2018**, *30*, 376–385.
- [32] F. Zhang, H. Ren, J. Dou, G. Tong, Y. Deng, *Sci. Rep.* **2017**, *7*, 40096.
- [33] N. Lin, A. Gèze, D. Wouessidjewe, J. Huang, A. Dufresne, *ACS Appl. Mater. Interfaces* **2016**, *8*, 6880–6889.
- [34] J. T. Korhonen, P. Hiekkataipale, J. Malm, M. Karppinen, O. Ikkala, R. H. A. Ras, *ACS Nano* **2011**, *5*, 1967–1974.
- [35] A. E. Way, L. Hsu, K. Shanmuganathan, C. Weder, S. J. Rowan, *ACS Macro Lett.* **2012**, *1*, 1001–1006.
- [36] Y. Kobayashi, T. Saito, A. Isogai, *Angew. Chem. Int. Ed.* **2014**, *53*, 10394–10397.
- [37] K. J. De France, K. J. W. Chan, E. D. Cranston, T. Hoare, *Biomacromolecules* **2016**, *17*, 649–660.
- [38] S. Sultan, A. P. Mathew, *Nanoscale* **2018**, *10*, 4421–4431.
- [39] B. Odell, M. V Reddington, A. M. Z. Slawin, N. Spencer, J. F. Stoddart, D. J. Williams, *Angew. Chem. Int. Ed.* **1988**, *27*, 1547–1550.
- [40] E. Córdova, R. A. Bissell, N. Spencer, P. R. Ashton, J. F. Stoddart, A. E. Kaifer, *J. Org. Chem.* **1993**, *58*, 6550–6552.
- [41] R. Castro, K. R. Nixon, J. D. Evanseck, A. E. Kaifer, *J. Org. Chem.* **1996**, *61*, 7298–7303.
- [42] S. Nygaard, K. C.-F. Leung, I. Aprahamian, T. Ikeda, S. Saha, B. W. Laursen, S.-Y. Kim, S. W. Hansen, P. C. Stein, A. H. Flood, et al., *J. Am. Chem. Soc.* **2007**, *129*, 960–970.
- [43] P. L. Anelli, P. R. Ashton, R. Ballardini, V. Balzani, M. Delgado, M. T. Gandolfi, T. T. Goodnow, A. E. Kaifer, D. Philp, *J. Am. Chem. Soc.* **1992**, *114*, 193–218.
- [44] C. H. Sue, S. Basu, A. C. Fahrenbach, A. K. Shveyd, S. K. Dey, Y. Y. Botros, J. F. Stoddart, *Chem. Sci.* **2010**, *1*, 119–125.
- [45] M. Bria, G. Cooke, A. Cooper, J. F. Garety, S. G. Hewage, M. Nutley, G. Rabani, P. Woisel, *Tetrahedron Lett.* **2007**, *48*, 301–304.
- [46] Complex **G1**⊂**CBPQT**⁴⁺ was prepared at [host] = [guest] = 5 × 10⁻³ M. **CNC-G1**⊂**CBPQT**⁴⁺ gel (2 mL) was obtained and solvent-exchanged inside a

UV-vis cuvette (10 mm pathlength); [host] $\approx 1.9 \times 10^{-3}$ M. The shown UV-vis spectrum of CNC-**G1**⊂**CBPQT**⁴⁺ was collected at $t = 31$ h after the addition of **G1**. Full data set is shown in Fig. S9a.

- [47] This molar ratio was chosen to facilitate the spectroscopic detection of both guests by ¹H NMR spectroscopy.